ELSEVIER

Journal of Molecular Structure (Theochem) 664-665 (2003) 279–289

THEO CHEM

www.elsevier.com/locate/theochem

A theoretical study of the gas-phase ion pair S_N2 reactions of lithium halide and methyl halide with inversion and retention mechanisms

Yan Xiong[a], Hua-jie Zhu[b,*], Yi Ren[a,*]

[a]*Faculty of Chemistry, Sichuan University, Chengdu 610064, People's Republic of China*
[b]*State Key Lab of Phytochemistry and Plant Resources in West China, CAS, Kunming, 650200, People's Republic of China*

Received 24 June 2003; revised 8 August 2003; accepted 1 October 2003

Abstract

Identity and non-identity ion pair S_N2 reactions, $LiX + CH_3X$, $LiY + CH_3X$ (Y, X = F, Cl, Br and I) were investigated using CCSD(T) calculations. Two possible reaction mechanisms, inversion and retention, were discussed. Introduction of lithium cation will significantly raise the inversion barriers and may lower the retention barriers. The analysis of barrier gaps between the two channels indicates that the retention mechanism is favorable for all of the reactions involving fluorine, in contrast to the anionic S_N2 reactions at carbon where inversion reaction pathway is much more favorable for all halogens. The stabilization energies for dipole–dipole complexes $CH_3X\cdots LiY$ (Y = F–I) are found to have a good correlation with the electronegativity of X. The CCSD(T) central barriers and overall barriers show good agreement with the predictions of Marcus equation and its modification, respectively. Further interesting feature of the non-identity ion pair S_N2 reactions is a good correlation between inversion central barriers and the composite geometric looseness (%L).

Keywords: Ion pair; S_N2 reaction; Identity and non-identity; Inversion and retention

1. Introduction

Bimolecular nucleophilic substitution (S_N2) is one of the most important reactions in chemistry and has played an important role in the development of modern physical organic chemistry [1,2]. Many theoretical efforts have been devoted to the gas phase anionic reactions in aliphatic systems [3]. However, most of the S_N2 reactions are carried out in the solution phase and the actual reactants involve neutral ion pair, which is the source of the anionic nucleophile. It appears that the ion pair reactions have been much less studied even though ion pairing is known to change the order of reactivity of halide ions [4]. Recently, a few theoretical studies have been done on the ion pair S_N2 reactions at carbon. Harder and Streitwieser et al. [5,6] studied the mechanism of ion pair S_N2 reactions MX + RX (M = Li, Na; R = Alkyl; X = F, Cl). They proposed two different reaction channels, inversion and

* Corresponding author. Tel.: +86-28-85412800; fax: +86-28-85257397.
E-mail addresses: yiren57@hotmail.com (Y. Ren);hjzh@mail.kib.ac.cn (H. Zhu).

0166-1280/$ - see front matter © 2003 Elsevier B.V. All rights reserved.
doi:10.1016/j.theochem.2003.10.002

retention. The calculated identity reactions of the methyl halides with lithium and sodium halides involve preliminary encounter dipole–dipole complexes instead of a negatively charged ion–dipole complex in anionic S_N2 reactions, then proceed via a cyclic inversion or retention transition structure with highly bent X–C–X bonds behaving as assemblies of ions.

In order to systematically investigate the fundamental gas-phase ion pair S_N2 reactions at carbon and compare the similarities and differences between the ion pair and anionic S_N2 reactions, following sets of reactions (Eqs. (1) and (2)) were examined

$$LiX + CH_3X \rightarrow CH_3X + LiX \quad (X = F, Cl, Br \text{ and } I) \tag{1}$$

$$LiY + CH_3X \rightarrow CH_3Y + LiX \quad (Y, X = F, Cl, Br \text{ and } I) \tag{2}$$

The present work represents the first computational study of this fundamental ion pair S_N2 reactions for all of the halogens and will hopefully provide some useful energy parameters to guide further experimental studies. We also wish to test the applicability of Marcus theory [7–9] and the additivity postulate [8] for Eq. (2).

2. Methodology

The geometries of all the species were fully optimized using the hybrid density functional method B3LYP [10] with 6-311 + G(d,p) basis sets. All minimum and transition states were verified by vibrational frequency analysis. Un-scaled vibrational zero-point energies (ZPE) determined at the B3LYP/6-311 + G(d,p) level were included in the calculation of relative energies for the various species involved in Eqs. (1) and (2). It is well known that B3LYP functional supplies too low energy barriers for S_N2 anionic reactions in the gas phase due to overestimation of electron correlation effects for the TS. So, further single point CCSD(T) [11] calculations were performed on all B3LYP optimized structures, i.e. CCSD(T)/6-311 + G(d,p)//B3LYP/6-311 + G(d,p) +ZPE (hereafter designed CCSD(T)).

All electron (AE) calculations were run for the first and second row elements, while Hay and Wadt [12] effective core potentials (ECP) were used for the third and fourth row elements. Charge distributions were calculated by the natural population analyses (NPA) [13–16] at the B3LYP/6-311 + G(d,p) level. All calculations were performed using the GAUSSIAN 98 system of programs [17].

Throughout this paper, all inter-nuclear distances are in angstroms and all angles are in degrees. Relative energies correspond to enthalpy changes at 0 K[ΔH (0 K)] in kJ/mol.

3. Results and discussion

The potential energy profile for the gas phase identity and non-identity reactions between methyl halide and lithium halide is described by a symmetrical double-well potential curve for the identity reactions or an asymmetric double-well potential curve for the non-identity reactions, which are the characters for all of the classic S_N2 reactions [2]. The reaction involves the initial formation of a reactant dipole–dipole complex **1**. This complex must then overcome the central activation barrier to reach an inversion transition structure **2** or retention transition structure **2′**. The latter then breaks down to give the product dipole–dipole complex, **3**, which subsequently dissociates into the separate products.

The key energetic quantities involved in reactions (Eq. (2)), as depicted in Fig. 1, are labeled as follows: ΔH_{YX}^{comp} and ΔH_{XY}^{comp} are the complexation energies for the dipole–dipole complex **1** and **3**, respectively. $\Delta H_{YX}^{\neq}$ and $\Delta H_{XY}^{\neq}$ are the central activation barriers, ΔH_{YX}^{b} and ΔH_{XY}^{b} are the overall activation barriers for the corresponding forward and reverse reaction. ΔH is the central enthalpy difference between the product and reactant ion–molecule complex **1** and **3**. ΔH^{ovr} is the overall enthalpy change for the forward reaction.

3.1. Reactants

The predicted properties of LiX (X = F–I) are compared with the MP2 [5] and the experimental results [18,19] in Table 1. The bond lengths at the level of B3LYP/6-311 + G(d, p) are very close to the experimental data and the mean signed error (MSE) is

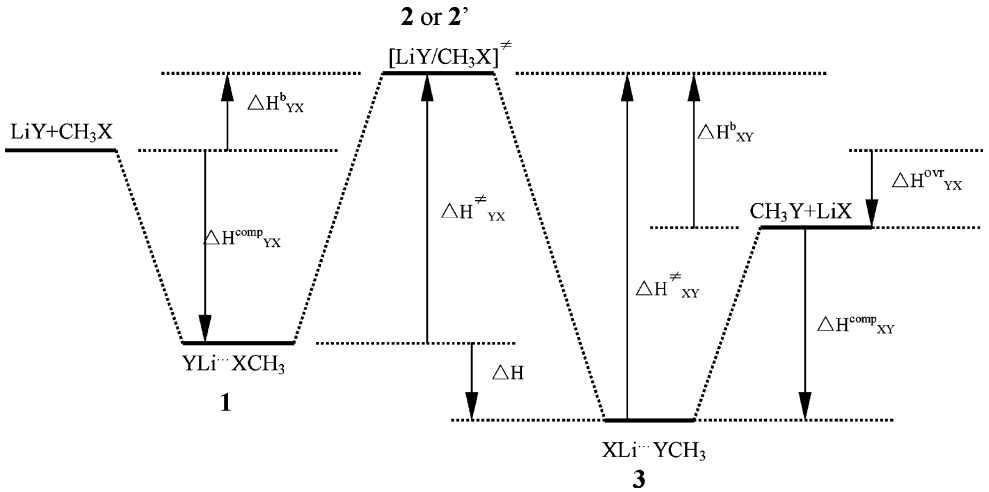

Fig. 1. Schematic energy profile for the LiY + CH_3X non-identity exchange reactions (Y,X = F–I).

only 0.012 Å. The harmonic vibrational frequencies and dipole moment obtained in the B3LYP method are also in good agreement with the experimental results.

The geometrical parameters for CH_3X (X = F–I) are listed in Table 2. The theoretical C–X bond lengths here generally agree well with the previous results of G2(+) theory [20] and experiments [21–24]. Comparing with the experimental data, the MSE for the C–X bond lengths in CH_3X is 0.026 Å while the largest deviation for the C–H bond lengths is 0.006 Å (for CH_3F). The calculated X–C–H angles differ from experimental values by up to 1.0° (X = I).

The NPA shows that F atom in CH_3F bears considerable negative charge (−0.39 e), in contrast to the situation for the other CH_3X molecules where chlorine has −0.1 e charge, bromine and iodine have almost zero charge.

3.2. Dipole–dipole complexes

For the ion pair S_N2 reactions of LiX + CH_3X and LiY + CH_3X, there are two possible conformers for the dipole–dipole complexes. The first form places the lithium cation in complexing with the

Table 1
Properties of LiX (X = F,Cl,Br and I)

Species	Level	r (Li–Y)	ν (cm^{-1})	μ (Dye)	D_{Li-X} (kJ/mol)
LiF	CCSD(T)[a]	1.583	898	6.360	528.9
	MP2/6-31 + G(d)[b]	1.588			
	Exp.[c]	1.564	910	6.284	577.0(± 21)[d]
LiCl	CCSD(T)	2.025	640	7.087	436.4
	MP2/6-31 + G(d)[a]	2.056			
	Exp.	2.021	643	7.085	469.0(± 13)
LiBr	CCSD(T)-ECP	2.191	555	7.210	389.4
	Exp.	2.170	563	7.226	418.8(± 4.2)
LiI	CCSD(T)-ECP	2.395	497	7.329	343.1
	Exp.	2.392	498	7.428	345.2(± 4.2)

[a] Geometries are optimized at the level of B3LYP/6-311 + G(d,p).
[b] From Ref. [6].
[c] From Ref. [18].
[d] From Ref. [19].

Table 2
Geometries and dipole moments for CH_3X and the dissociation energies for bonds C–X in CH_3X(X = F, Cl, Br, and I)

	Level	r(C–X)	r(C–H)	∠X–C–H	μ(Dye)	$Dc - x$(*kJ/mol*)
CH_3F	CCSD(T)	1.396	1.092	108.6	2.085	420.2
	G2(+)[a]	1.407	1.090	108.0		463.0
	Exp.[b]	1.383	1.086	108.8	1.858[c]	465.4[d]
CH_3Cl	CCSD(T)	1.806	1.087	108.3	2.106	316.6
	G2(+)	1.780	1.089	108.9		347.3
	Exp.[e]	1.776	1.085	108.6	1.892[c]	342.0
CH_3Br	CCSD(T)-ECP	1.969	1.086	107.7	2.026	267.7
	G2(+)-ECP	1.954	1.088	108.0		285.9
	Exp.[f]	1.934	1.082	107.7	1.822[c]	289.9
CH_3I	CCSD(T)-ECP	2.159	1.085	107.6	1.793	227.4
	G2(+)-ECP	2.140	1.088	108.0		237.0
	Exp.[g]	2.132[c]	1.085[c]	108.6[c]	1.620[c]	231.2[i]

[a] At the MP2(fc)/6-31 + G(d), from Ref. [26].
[b] From Ref. [21].
[c] From Ref. [19], **9**–18 ~ **9**–21.
[d] From Ref. [18].
[e] From Ref. [22].
[f] From Ref. [23].
[g] From Ref. [24].

halogen at CH_3X to form a so-called 'X-philic' pre-reaction complex $CH_3X\cdots LiY$. In the alternative complexes, the halogen can coordinate with the carbon and three hydrogen atoms to form the complex $LiY\cdots CH_3X$, similar to the one in anionic S_N2 reaction, which are found to be much higher in energy than the X-philic complex. For example, at the B3LYP/6-311 + G(d, p) + ΔZPVE level, the energy of $CH_3F\cdots LiF$ is lower than $LiF\cdots CH_3F$ by 56.6 kJ/mol, while $CH_3Cl\cdots LiCl$ is lower than $LiCl\cdots CH_3Cl$ by 40.3 kJ/mol. Therefore, only X-philic complex is considered here.

The effects of $CH_3X\cdots LiY$ complexation are two-fold: (1) it increases the C–X bond distance in the free reactants from 1.396 to about 1.44 Å (X = F), 1.806 to about 1.84 Å (X = Cl), 1.970 to 2.00 Å (X = Br) and 2.159 to 2.18 Å (X = I). (2) it increases the effective charge on the CH_3 group from +0.39 to about +0.46e for X = F, +0.08 to +0.16e for X = Cl, 0.00–0.08 e for X = Br and −0.10 to −0.01e for X = I, respectively, that are favorable for the proceeding of the subsequent nucleophile attack.

The set of complexation enthalpies in Table 3 indicates that the complexation enthalpies depend primarily on the identity of substrate CH_3X, and only to a small extent on the identity of nucleophile LiY and tend to decrease in the order: $CH_3F > CH_3Cl > CH_3Br > CH_3I$, in contrast to those found for non-identity anionic S_N2 reactions at carbon [25], where complexation energies for $Y^-\cdots CH_3X$ depend primarily on the identity of nucleophile Y^-. That suggests that the interaction between lithium cation and halogen atom on CH_3X dominants the stabilization energy. Thus, the complexation energies for CH_3F range between 63.3 and 69.8 kJ/mol, those for CH_3Cl range between 60.4 and 63.5 kJ/mol, those for CH_3Br range between 55.0 and 57.2 kJ/mol, while those for CH_3I range between 52.0 and 54.6 kJ/mol.

CCSD(T) complexation energies for complexes $CH_3X\cdots LiY$(Y, X = F–I), ΔH_{YX}^{comp} and ΔH_{XY}^{comp}, are scattered with a range of 17.8 kJ/mol because of close dipole–dipole interactions between both participating species, which is smaller than the corresponding range ca. 29 kJ/mol for ion–dipole complexes $Y^-\cdots H_3CX$ (Y, X = F–I) at the G2(+) level [25]. These complexation energies for $H_3CX\cdots LiY$ show reasonable linear relationships

Table 3
Energetics (kJ/mol) of the $LiY + CH_3X \rightarrow CH_3Y + LiX$ reactions

Y, X	ΔH_{YX}^{comp}	$\Delta H_{YX}^{\neq}$		ΔH_{YX}^{b}		ΔH_{XY}^{b}		$\Delta H_{XY}^{\neq}$		ΔH_{XY}^{comp}	ΔH	ΔH^{ovr}
		inv.	ret.	inv.	ret.	inv.	ret.	inv.	ret.			
F, F	63.3(56.5)[a]	269.1(48.5)	205.6(241.0)	205.7(−8.0)	142.2(184.5)							
Cl, Cl	62.6(44.0)	214.6(55.5)	215.3(237.8)	152.0(10.3)	152.7(193.8)							
Br, Br	56.7(41.1)	177.2(46.9)	198.7(220.0)	120.5(5.8)	142.0(178.9)							
I, I	54.6(36.0)	151.4(42.5)	191.7(207.4)	96.8(6.5)	137.1(171.4)							
F, Cl	60.4(64.4)	232.4(11.9)	200.8	172.0(−52.5)	140.4	183.1(75.0)	151.5	251.1(114.3)	219.5	67.9(39.3)	−18.7(−102.4)	−11.2(−127.5)
		232.6[b]	**201.2**	**173.3**	**141.9**	**184.5**	**153.4**	**251.2**	**220.0**			
F, Br	55.0(68.9)	209.3(3.1)	188.2	154.3(−65.8)	133.2	169.2(93.8)	148.1	238.0(128.4)	216.9	68.8(34.6)	−28.7(−125.3)	−14.9(−159.6)
		209.0	**188.0**	**155.7**	**134.7**	**170.6**	**149.6**	**237.7**	**216.8**			
F, I	52.0(69.6)	198.2(0.8)	186.4	146.2(−68.9)	134.3	154.2(109.0)	142.3	224.0 (139.7)	212.2	69.8(30.7)	−25.8(−138.9)	−8.0(−177.5)
		197.5	**186.0**	**147.3**	**135.7**	**155.3**	**143.7**	**223.3**	**211.8**			
Cl, Br	56.4(46.3)	190.6(39.5)	201.6	134.2(−6.8)	145.2	137.9(25.3)	148.9	201.1(64.3)	212.1	63.2(39.0)	−10.5(−24.8)	−3.7(−32.1)
		190.7	**201.8**	**134.4**	**145.5**	**138.1**	**149.2**	**201.2**	**212.3**			
Cl, I	53.6(45.8)	179.6(32.0)	200.6	126.0(−13.8)	146.9	122.8(36.2)	143.8	186.4(70.6)	207.3	63.5(34.4)	−6.8(−38.6)	3.2(−49.9)
		179.6	**200.1**	**126.0**	**146.5**	**122.8**	**143.2**	**186.4**	**206.9**			
Br, I	54.2(40.7)	166.3(38.4)	197.2	112.2(−2.3)	143.1	105.3(15.6)	136.2	162.5(51.9)	193.4	57.2(36.3)	3.8(−13.5)	6.9(−17.9)
		166.2	**197.1**	**112.1**	**143.0**	**105.2**	**136.1**	**162.4**	**193.3**			

[a] Values in parentheses are corresponding energetics at the G2(+) level for the reactions $X^- + CH_3X$ and $Y^- + CH_3X$.
[b] Values in bold are the calculated central barriers with Eq. (9) and overall barriers with Eq. (10).

with the electronegativity of X using Mulliken scale ($R^2 > 0.88$), which are analogous to those found in the anionic S_N2 reactions [26].

3.3. Transition state structures and central barrier heights

3.3.1. Geometries of transition states

The most important geometrical features in the inversion LiX/CH_3X or LiY/CH_3X TS are remarkable deformation from the linear structures found in anionic S_N2 reactions at carbon. The bridging of Li cation causes a large decerase of Y–C–X angles by 90–110°. For example, the F–C–Cl and Br–C–I angles decrease from 180 to 94.9°, 109.4° for the inversion LiF/CH_3Cl and $LiBr/CH_3I$ TS, respectively. The significantly deformation of TS structure may be responsible for the much higher central barrier for the ion pair reaction than the corresponding anionic S_N2 reaction [20,25]. The decrease of angle Y–C–X will increase the electrostatic repulsion between $Y^-\cdots X^-$ and thus destabilize the ion pair TS relative to the anionic TS. In contrast, smaller geometries changes relative to anionic S_N2 TS with retention of configuration [26] are observed for the retention LiX/CH_3X TS. For example, in the retention LiX/CH_3X TS, the X–C–X angles are in a smaller range from 75.9(X = F) to 88.7°(X = I), which are close to the angles in anionic TS, varying from 80.9(X = F) to 87.1°(X = I). The geometrical similarities of retention transition structures will lead to a smaller barrier difference between the ion pair and anionic reactions.

The other geometrical features in both of the inversion LiX/CH_3X or LiY/CH_3X TS are the elongation of bond C–X and Li–Y relative to dipole–dipole complexes. We can easily characterize the looseness of the transition structure by geometrical looseness parameters $\%C-X^{\neq}$, $\%C-Y^{\neq}$, $\%Li-X^{\neq}$, $\%Li-Y^{\neq}$ and the composite transition structure looseness $\%L^{\neq}$ in a similar way to that proposed by Shaik et al. [2].

$$\%C - X^{\neq} = 100[r^{\neq}_{C-X} - r^{comp}_{C-X}]/r^{comp}_{C-X} \quad (3)$$

$$\%C - Y^{\neq} = 100[r^{\neq}_{C-Y} - r^{comp}_{C-Y}]/r^{comp}_{C-Y} \quad (4)$$

$$\%Li - X^{\neq} = 100[r^{\neq}_{Li-X} - r^{comp}_{Li-X}]/r^{comp}_{Li-X} \quad (5)$$

$$\%Li - Y^{\neq} = 100[r^{\neq}_{Li-Y} - r^{comp}_{Li-Y}]/r^{comp}_{Li-Y} \quad (6)$$

$$\%L^{\neq} = \%C - X^{\neq} + \%C - Y^{\neq} + \%Li - X^{\neq} + \%Li - Y^{\neq} \quad (7)$$

where $r^{\neq}_{C-X}$, $r^{\neq}_{C-Y}$, $r^{\neq}_{Li-X}$, $r^{\neq}_{Li-Y}$ and r^{comp}_{C-X}, r^{comp}_{C-Y}, r^{comp}_{Li-X}, r^{comp}_{Li-Y} are the C–X, C–Y, Li–X, Li–Y bond lengths in the transition structure **2** or **2′** and the dipole–dipole complex **1** or **3**, respectively.

The $\%L^{\neq}$ values for **2** lie within in a larger range of 24.5 than corresponding value of just 2.9 for **2′**. The geometric looseness parameters for the inversion and retention transition structures are presented in Fig. 2.

3.4. Barrier heights

All of the inversion central barriers, $\Delta H^{\neq}_{YX}(inv)$ and $\Delta H^{\neq}_{XY}(inv)$, for the non-identity ion pair reactions $LiY + CH_3X \rightarrow CH_3Y + LiX$ (Y,X = F–I) at the CCSD(T) level are much larger than the corresponding data in the anionic S_N2 reactions [25], ranging from 162.5 kJ/mol for Y = I, X = Br up to 251.1 kJ/mol for Y = Cl, X = F with an decrease of the Y–C–X angle and increase of the composite looseness index $\%L^{\neq}$. This large barrier range is also significantly greater than one in the corresponding anionic reactions (varying from 0.8 kJ/mol for Y = F, X = I to 39.5 kJ/mol for Y = Cl, X = Br) where all of the angle Y–C–X is 180° and the geometrical looseness for transition state vary in a small range from 48.2 to 59.3). The overall barriers, $\Delta H^{b}_{YX}(inv)$ and $\Delta H^{b}_{XY}(inv)$, for the reactions of $LiY + CH_3X$ (Y, X = F–I) are all positive, varying from 105.3 kJ/mol for Y = I, X = Br up to 183.1 kJ/mol for Y = Cl, X = F, in contrast to those for the non-identity anionic S_N2 reactions [25] where all of the inversion overall barriers are negative, varying from −68.9 kJ/mol for Y = F, X = I to −2.3 kJ/mol for Y = Br, X = I. This indicates that the inclusion of Li in the anionic S_N2 reactions will raise the inversion barrier heights by strongly deforming of its idea linear geometry. Therefore, LiX is much less reactive than X^- for the inversion mechanism with CH_3X.

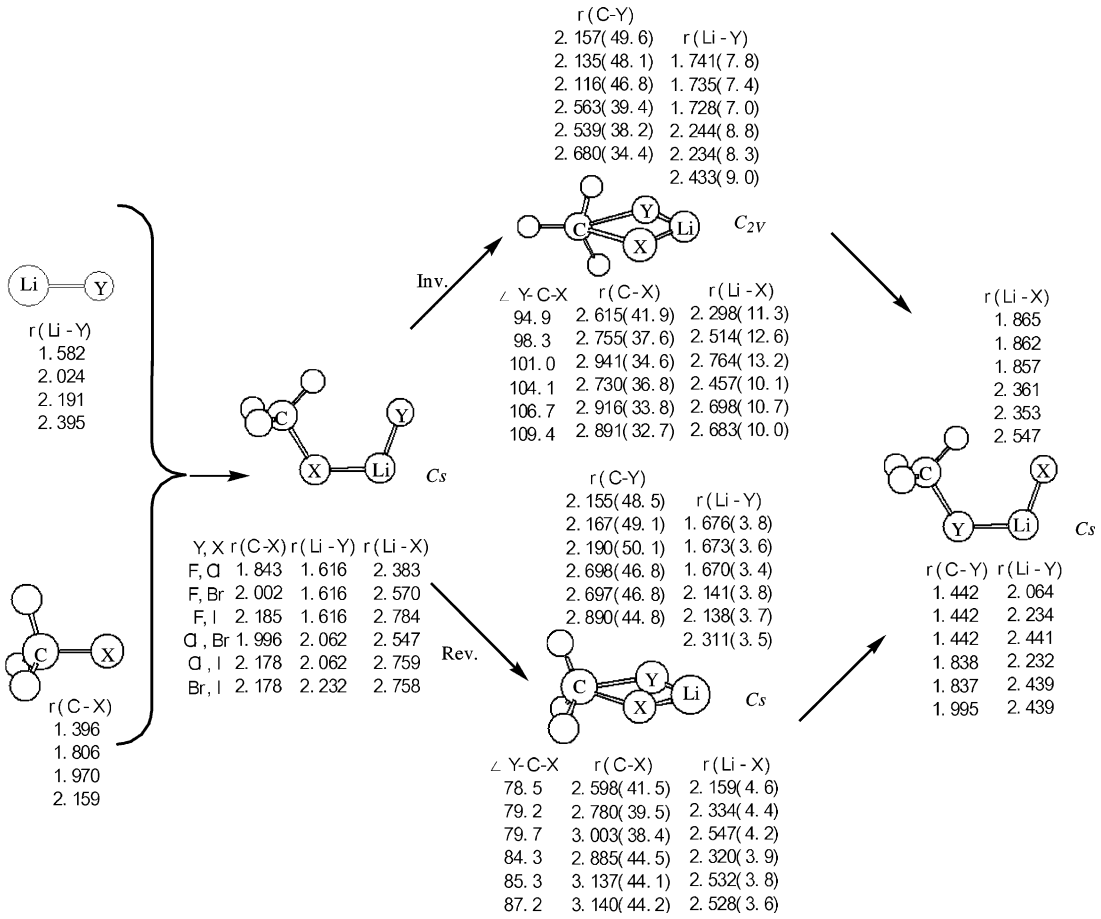

Fig. 2. B3LYP/6-311 + G(d,p) optimized geometries for all the species in Eq. (2), the data in parentheses are the geometric looseness of the TSs.

The central barriers and overall barriers of the $LiX + CH_3X(X = F–I)$ reactions for retention channel, $\Delta H^{\neq}_{XX}$(ret) and ΔH^{b}_{XX}(ret), vary within a relatively narrow range of just 23.6 and 15.6 kJ/mol, respectively, that are close to the previous study on the identity gas-phase S_N2 reactions $X^- + CH_3X$ $(X = F–I)$ with retention of configuration [26]. These barrier heights, $\Delta H^{\neq}_{XX}$(ret) and ΔH^{b}_{XX}(ret), are found to be less than the corresponding values in the $X^- + CH_3X$ $(X = F–I)$ reactions. That may imply that the presence of Li in the anionic S_N2 reactions will lower the energy of retention TS by the triple ion LiX_2^- stabilization [5].

As can be seen from the Table 3, for the ion pair S_N2 reactions involving the fluorine, all of the inversion central barriers or overall barriers are larger than corresponding values in the retention mechanism, which is in agreement with the conclusion of Harder et al. [5]. That indicates that the retention mechanism is favorable in energy compared to the inverse for the reactions $LiF + CH_3X$ $(X = F–I)$ and their reverse, and the inversion mechanism is favored for other reactions $LiY + CH_3X$ (Y, X = Cl, Br and I).

The data in Table 3 also show that if the reactions are exothermic, the central barrier heights are lower than the intrinsic central barrier $\Delta H^{\neq}_{0\,YX}$, while the central barrier heights for those endothermic reactions are higher than $\Delta H^{\neq}_{0\,YX}$. These results are all expected since the identity reactions are thermoneutral.

According to the Marcus theory [7,9], in an exothermic reaction, a thermodynamic driving force will lower the transition state energy, whereas endothermic reactions will induce a higher activation energy. $\Delta H^{\neq}_{0\ YX}$ is estimated using the additivity postulate [15]:

$$\Delta H^{\neq}_{0\ YX} = 0.5[\Delta H^{\neq}_{YY} + \Delta H^{\neq}_{XX}] \quad (8)$$

in which $\Delta H^{\neq}_{YY}$ and $\Delta H^{\neq}_{XX}$ are the central barriers for the identity S_N2 reactions.

3.5. Correlation of barrier heights

There has been considerable discussing in the literature as to what factors might influence the barrier heights in the gas phase anionic S_N2 reaction [2,20,25,27,28]. In this context, we will briefly discuss our computational data for ion pair substitution at carbon. We will seek the relationship between the central barriers with reactant properties, geometrical and energetic characteristics of the transition structures, and check whether the reactions of LiY with CH_3X show similar pattern of behavior to the anionic one.

The calculation of the anionic non-identity S_N2 reactions $Y^- + CH_3X$ (Y, X = F, Cl, Br and I) at the G2(+) level shows a reasonable correlation between the central barriers and the composite transition structure looseness, $\%L^{\neq}$ ($R^2 = 0.821$) [25]. In the ion pair S_N2 reactions $LiY + CH_3X$ (Y, X = F–I), a good linear relationship between the central barriers with the composite looseness of the S_N2 transition structures $\%L^{\neq}$ (Fig. 3, $R^2 = 0.964$) is observed for the inversion mechanism, bur breaks down for the retention mechanism.

Inspection of Tables 1 and 3 indicates that there are correlations between the bond dissociation energies D_{C-X} ($R^2 \approx 0.995$, Fig. 4) and the inversion central barriers for the reactions $LiY + CH_3X$, where Y is fixed, X = F, Cl, Br and I, respectively. Meanwhile, the bond dissociation energies, D_{Li-Y}, exhibit good correlations with the inversion central barriers for the reactions $LiY + CH_3X$, where X is fixed, Y = F, Cl, Br and I, respectively, ($R^2 \approx 0.986$, Fig. 5).

Marcus theory has been successfully applied to the interpretation of gas-phase anionic S_N2 reactions at carbon [25] and oxygen [28]. It will be interesting to test the reliability of the Marcus theory for the ion pair S_N2 reactions. The Marcus equation (Eq. (9)) relates the

$$\Delta H^{\neq}_{YX} = \Delta H^{\neq}_{0\ YX} + 0.5\Delta H + [(\Delta H)^2/16\Delta H^{\neq}_{0\ YX}] \quad (9)$$

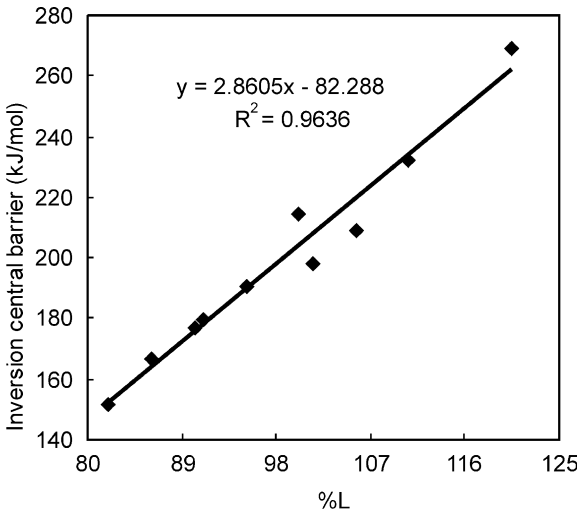

Fig. 3. Plot of CCSD(T) central barriers of inversion pathway for forward reactions (Table 3) vs. the composite geometric looseness of inversion LiX/CH_3X TS (%L) (Eq. (7)).

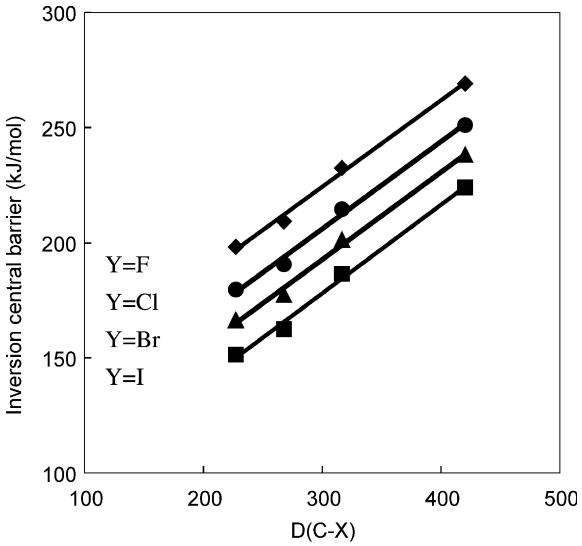

Fig. 4. Plots of CCSD(T) central barriers for inversion LiY/CH_3X TS(X = F–I) vs. the dissociation energies of C–X bond in CH_3X (D_{C-X}). The D_{C-X} values are listed in Table 2.

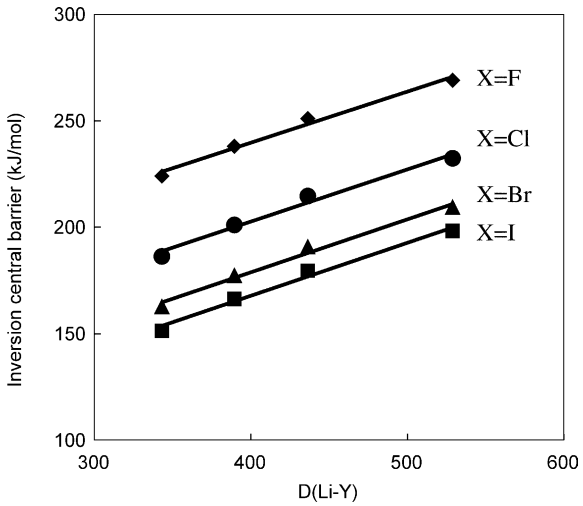

Fig. 5. Plots of CCSD(T) central barriers for inversion LiY/CH_3X TS(Y = F–I) vs. the dissociation energies of Li–Y bond (D_{Li-Y}). The D_{Li-Y} values are listed in Table 1.

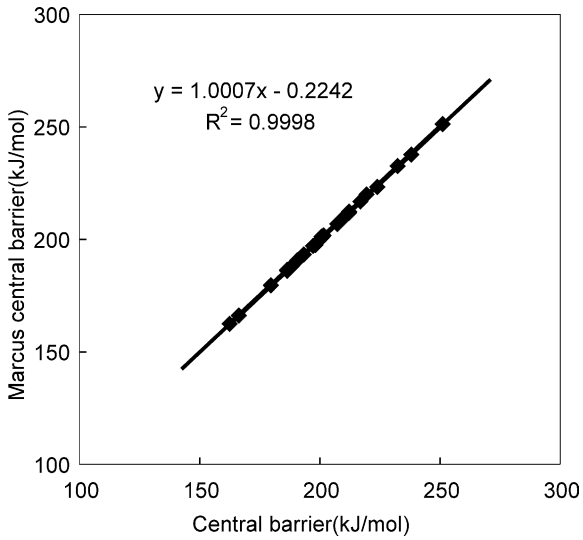

Fig. 6. Plot of central barriers from Eq. (9) vs. the same quantity obtained directly from the CCSD(T) calculations (Y, X = F, Cl, Br, I). The values are listed in Table 3.

intrinsic barrier height of a non-identity substitution reaction to the corresponding intrinsic barrier heights in the absence of a thermodynamic driving force and the central enthalpy difference between product and reactant ion-molecule complex **3** and **1**. It is seen from Table 3 that the barrier heights predicted by Marcus theory are within a few kJ/mol of the actual CCSD(T) computed values no matter inversion or retention channel, the largest difference being only 0.7 kJ/mol. A plot of barriers calculated according to Eq. (9) vs. the corresponding CCSD(T) data gives a very good correlation (Fig. 6, $R^2 = 1.000$).

Since the property that is measured experimentally in a gas phase S_N2 reaction is the overall barrier, rather than the central barrier, Wolfe et al. [29] proposed the following modifications

$$\Delta H^{b}_{YX} = \Delta H^{b}_{0\,YX} + 0.5\Delta H_{ovr} + [(\Delta H_{ovr})^2/16\Delta H^{\neq}_{0\,YX}] \quad (10)$$

$$\Delta H^{b}_{0\,YX} = 0.5[\Delta H^{b}_{YY} + \Delta H^{b}_{XX}] \quad (11)$$

Eq. (10) facilitates predictions of experimentally more accessible quantities from data for the corresponding identity reactions. Most of the values derived from Eq. (10) are a little bit higher than the calculated CCSD(T) results and the MSE is 0.7 kJ/mol. This good estimation can be attributed to the smaller exothermicity or endothermicity for the LiY + CH_3X (Y, X = F– I) reactions (Table 3). Fig. 6, a plot of $\Delta H^{b}_{\ YX}$ deduced by Eq. (10) versus ΔH^{b}_{YX} computed by the CCSD(T) method, illustrates the applicability of Wolfe et al. modification to the Marcus equation for the ion pair S_N2 reaction at carbon ($R^2 = 0.999$). (Fig. 7)

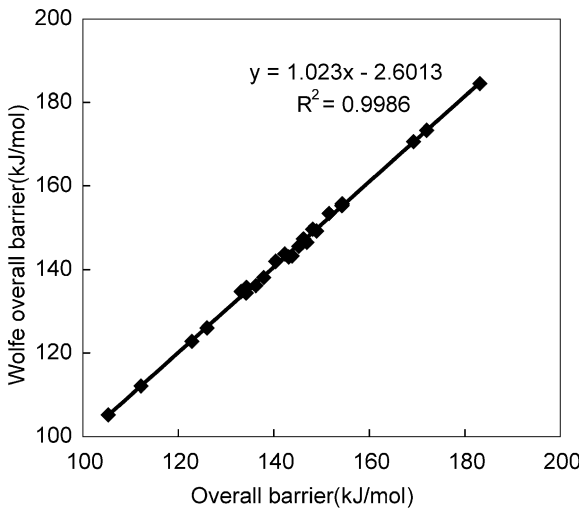

Fig. 7. Plot of overall barriers from Eq. (10) vs. the same quantity obtained directly from the CCSD(T) calculations (Y, X = F, Cl, Br and I). The values are listed in Table 3.

4. Conclusions

Theoretical investigation of the gas-phase non-identity ion pair exchange reactions at saturated carbon $LiX + CH_3X \rightarrow LiX + CH_3Y$ and $LiY + CH_3X \rightarrow LiX + CH_3Y$ (Y, X = F, Cl, Br and I) using CCSD(T) calculations leads to the following conclusions

(1) There are two possible pathways via the same $CH_3X\cdots LiY$ complex and different transition structures, inversion or retention. The energy profiles for the identity and non-identity exchange reactions are described by a symmetric or an asymmetric double-well curve, with the following pathway

$$CH_3X + LiX \rightarrow CH_3X\cdots LiX \rightarrow [LiX/CH_3X]^{\neq} \rightarrow XLi\cdots XCH_3 \rightarrow LiYX + CH_3X$$

$$CH_3X + LiY \rightarrow CH_3X\cdots LiY \rightarrow [LiY/CH_3X]^{\neq} \rightarrow XLi\cdots YCH_3 \rightarrow LiY + CH_3X$$

(2) Introduction of the lithium cation will significantly raise the inversion barriers and may lower the retention central barriers for the ion pair S_N2 reactions.

(3) The energies gaps $[\Delta H^b_{YX}(\text{ret}) - \Delta H^b_{YX}(\text{inv})]$ or $[\Delta H^b_{XY}(ret) - \Delta H^b_{XY}(\text{inv})]$ suggest the retention mechanism are favorable for the ion pair S_N2 reactions involving fluorine and the inversion mechanism are favored for the other reactions.

(4) Complexation enthalpies of dipole–dipole complexes $CH_3X\cdots LiY$ depend primarily on the identity of X and are found to correlate well with the electronegativity of X.

(5) There are good correlations between CCSD(T) inversion central barriers and the composite geometrical looseness of the transition state ($\%L^{\neq}$) and inversion overall barriers. For the reactions $LiY + CH_3X$ (X = F– I), inversion central barriers demonstrate good correlations with the bond dissociation energies D_{C-X}. As for the reactions $LiY + CH_3X$ (Y = F–I), inversion central barriers also give good correlations with the bond dissociation energies D_{Li-Y}. These correlations break down for the retention mechanism.

(6) The set of non-identity reactions $LiY + CH_3X$ (Y, X = F–I) obeys the Marcus equation and its modification. The central barriers estimated from the Marcus equation and the overall barriers obtained from Wolfe equation are very close to the directly calculated CCSD(T) barriers and plots of the data sets give good correlations ($R^2 = 1.000$ for central barriers and $R^2 = 0.999$ for overall barriers).

5. Supporting information available

Calculated NPA charge of species involved in the ion pair S_N2 reactions. This material is available free of charge via the Internet.

Acknowledgements

The authors in Sichuan University are thankful for the support from the Scientific Research Foundation for the Returned Chinese Scholars of State Education Ministry. H.J. Zhu thanks the support of 'Bairenjihua' Fund from CAS and the Fund (NSFC#20242012). We express our gratitude to the referee of their valuable comments.

References

[1] T.H. Lowry, K.S. Richardson, Mechanism and Theory in Organic Chemistry, third ed., Harper and Row, New York, 1987.
[2] S.S. Shaik, H.B. Schlegel, S. Wolfe, Theoretical Aspects of Physical Organic Chemistry, The S_N2 Mechanism, Wiley, New York, 1992.
[3] J.K. Laerdahl, E. Uggerud, Int. J. Mass Spectrom. 214 (2002) 277 (and references cited therein).
[4] S. Winstein, L.G. Savedoff, S. Smith, I.D.R. Stevens, J.S. Gall, Tetrahedron Lett. (1960) 24.
[5] S. Harder, A. Streitwieser, J.T. Petty, P.v.R. Schleyer, J. Am. Chem. Soc. 117 (1995) 3253.
[6] A. Streitwieser, G.S-C. Choy, F. Abu-Hasanayn, J. Am. Chem. Soc. 119 (1997) 5013.
[7] R.A. Marcus, Annu. Rev. Phys. Chem. 15 (1964) 155.
[8] R.A. Marcus, J. Phys. Chem. 72 (1968) 891.
[9] W.J. Albery, Annu. Rev. Phys. Chem. 31 (1980) 227.
[10] C. Lee, W. Yang, R.G. Parr, Phys.Rev. B 37 (1988) 785.

[11] J.A. Pople, M. Head-Gordon, K. Raghavachari, J. Chem. Phys. 87 (1987) 5968.
[12] W. Wadt, P.J. Hay, J. Chem. Phys. 82 (1985) 284.
[13] A.E. Reed, R.B. Weinstock, F. Weinhold, J. Chem. Phys. 83 (1985) 735.
[14] J.P. Foster, F. Weinhold, J. Am. Chem. Soc. 102 (1980) 7211.
[15] A.E. Reed, F. Weinhold, J. Chem. Phys. 78 (1983) 4066.
[16] A.E. Reed, L.A. Curtiss, F. Weinhold, Chem. Rev. 88 (1988) 899.
[17] M.J. Frisch, G.W. Trucks, H.B. Schlegel, et al GAUSSIAN 98, Revision A.7; Gaussian, Inc.: Pittsburgh, PA, 1998.
[18] NIST Standard Reference Database Number 69, July 2001 Release (http://webbook.nist.gov/chemistry)
[19] D.R. Lide, CRC Handbook of Chemistry and Physics, 72th ed., CRC Press, Boca Patonand/Ann Arbor/Boston, 1991–1992.
[20] M.N. Glukhovtsev, A. Pross, L. Radom, J. Am. Chem. Soc. 117 (1995) 2024.
[21] T. Egawa, S. Yamamoto, M. Nakata, K. Kuchitsu, J. Mol. Struct. 156 (1987) 213.
[22] T. Jensen, S. Brodersen, G. Guelachvili, J. Mol. Spectrosc. 88 (1981) 378.
[23] G. Graner, J. Mol. Spectrosc. 90 (1981) 394.
[24] M.D. Hannonv, V.W. Laurie, R.L. Kuczkowski, D.A. Ramsav, F.J. Lovas, W.J. Lafferty, A.G. Maki, J. Phys. Chem. Ref. Data 8 (1979) 619.
[25] M.N. Glukhovtsev, A. Pross, L. Radom, J. Am. Chem. Soc. 118 (1996) 6273.
[26] M.N. Glukhovtsev, A. Pross, H.B. Schlegel, R.D. Bach, L. Radom, J. Am. Chem. Soc. 118 (1996) 11258.
[27] Y. Ren, J.L. Wolk, S. Hoz, Int. J. Mass Spectrom. 220 (2002) 1.
[28] Y. Ren, J.L. Wolk, S. Hoz, S. Int, J. Mass Spectrom. 225 (2003) 167.
[29] S. Wolfe, D.J. Mitchell, H.B. Schlegel, J. Am. Chem. Soc. 103 (1981) 76942.